Computers & Geosciences 46 (2012) 44–50

Contents lists available at SciVerse ScienceDirect

Computers & Geosciences

journal homepage: www.elsevier.com/locate/cageo

Impact of soil deformation on phreatic line in earth-fill dams

Yu-xin Jie [a,*], Yan-feng Wen [b], Gang Deng [b], Rui Chen [c], Ze-ping Xu [b]

[a] State Key Laboratory of Hydroscience and Engineering, Tsinghua University, Beijing 100084, China
[b] State Key Laboratory of Simulation and Regulation of Water Cycle in River Basin, China Institute of Water Resources and Hydropower Research, Beijing 100048, China
[c] Harbin Institute of Technology Shenzhen Graduate School, Shenzhen 518055, China

ARTICLE INFO

Article history:
Received 1 January 2012
Received in revised form
4 April 2012
Accepted 5 April 2012
Available online 12 April 2012

Keywords:
Seepage
Unsaturated soil
Consolidation
Earth-rock dam
Pore water pressure

ABSTRACT

Generally seepage analysis and stress–strain analysis are conducted separately in the analysis of dams with varied water levels, which neglects the impact of soil deformation on seepage. The impact, however, is significant when the water level varies greatly. In this study, a simplified approach for consolidation analysis of unsaturated soil is used to conduct numerical simulations of water-filling in an earth-rock dam. Pore water pressure and phreatic line are simultaneously obtained in addition to stress and displacement within the dam. The computational results show that due to the coupling effect between deformation and pore water pressure, the development of phreatic line within the core-wall of the dam is quicker than that computed from unsaturated seepage analysis without coupling deformation. The variations of pore water pressure are related not only to unsaturated seepage induced by variations of water level, but also to the excess pore water pressure induced by deformation.

1. Introduction

When a dam is subjected to varied water levels, its seepage analysis and stress–strain analysis are usually conducted separately. Seepage analysis is firstly carried out and subsequently followed by stress–strain analysis. Based on such an approach, the impact of stress–strain properties of soil on seepage is neglected. Seepage analysis is a classic topic in soil mechanics and it can be conducted by using many numerical methods such as the routine finite difference method, the finite-volume method, the boundary-fitted coordinate transformation method, the finite element method, the numerical manifold method, the meshless method etc. (Bathe and Khoshgoftaar, 1979; Darbandi et al., 2007; Desai, 1976; Jiang et al., 2010; Jie et al., 2004; Lam and Fredlund, 1984; Li et al., 2003; Zheng et al., 2005). The soil mass below the phreatic line is under saturated conditions with positive pore water pressure, then seepage theories for saturated soil are applicable. Regarding the soil mass above the phreatic line with negative pore water pressure, seepage theories for unsaturated soil are required and the coefficient of permeability varies with negative pore water pressure (Fredlund and Rahardjo, 1993).

If the variation in water level is small, it is generally believed that the seepage is marginally affected by the stress–strain properties of soil. However, when the water level varies greatly, the impact of stress–strain properties of soil on seepage cannot be neglected and consolidation theories are required. Biot's consolidation theory has been extensively used in the analysis of saturated soil (Biot, 1941; Sandhu and Wilson, 1969). However, if negative pore water pressure exits, the consolidation theories for unsaturated soil will be more suitable.

The consolidation model coupling deformation, pore water pressure and pore air pressure was first proposed by Barden (1965). Closed formulations were derived by using continuity equations of water and gas, Darcy's law, suction state function, Bishop's effective stress equation and the relationship between porosity and effective stress. Other typical consolidation formulations were proposed by Scott (1963), Lloret and Alonso (1980), and Fredlund et al. (Fredlund and Hasan, 1979; Fredlund and Morgenstern, 1976; Fredlund and Rahardjo, 1993).

In this paper, a simplified approach for consolidation analysis of unsaturated soil suggested by Shen (2003) is used to conduct consolidation analysis of an earth-rock dam subjected to water filling. This approach is based on Bishop's effective stress (Bishop, 1959). By introducing the air drainage ratio, pore air pressure can be solved indirectly and is no longer treated as an unknown quantity in governing equations, greatly simplifying the amount of computation and the complexity of programming. It has been successfully used to analyze surface cracks on clay by Deng and Shen (Deng et al., 2003, 2006; Deng and Shen, 2006). Here, this approach is employed to analyze the seepage in an earth-rock dam during water filling and to study the impact of deformation of soil on the development of phreatic line.

* Corresponding author. Tel./fax: +86 10 62785593.
E-mail address: jieyx@tsinghua.edu.cn (Y.X. Jie).

0098-3004/$ - see front matter © 2012 Elsevier Ltd. All rights reserved.
http://dx.doi.org/10.1016/j.cageo.2012.04.005

2. Methodology

2.1. Governing equations for consolidation analysis

To be consistent with the general mechanical analysis, sign convention used in elasticity mechanics is adopted in this section unless otherwise stated. Such sign convention is opposite to that generally used in soil mechanics. In order to assure the value of suction positive, suction is defined as $s=u_w-u_a$, different from the conventional definition $s=u_a-u_w$, where u_a is the pore air pressure and u_w is the pore water pressure.

Bishop's effective stress is adopted with its definition as follows:

$$\sigma'=\sigma-u_a+\chi(u_a-u_w) \tag{1}$$

where σ' is the effective stress and σ is the total stress. This expression is identical to that using sign convention in soil mechanics.

The above equation can be written as

$$\sigma=\sigma'+u_a-\chi(u_a-u_w) \tag{2}$$

Then we can get:

$$\Delta\sigma=\Delta\sigma'+\Delta u_a-\Delta\chi(-s)-\chi(\Delta u_a-\Delta u_w) \tag{3}$$

and

$$\Delta\chi=\frac{\partial\chi}{\partial s}\Delta s=\frac{\partial\chi}{\partial s}(\Delta u_w-\Delta u_a) \tag{4}$$

Substituting the above equation into Eq. (3) yields

$$\Delta\sigma=\Delta\sigma'+\left(1-\chi-\frac{\partial\chi}{\partial s}s\right)\Delta u_a+\left(\chi+\frac{\partial\chi}{\partial s}s\right)\Delta u_w \tag{5}$$

The above expression can also be derived by using sign convention in soil mechanics.

According to the simplified approach for consolidation analysis (Deng et al., 2003; Shen, 2003), pore air content (pore air volume in unit total soil volume) is defined as

$$n_a=[1-(1-c_h)S_r]n \tag{6}$$

where n is the porosity, S_r is the degree of saturation and c_h is the volumetric coefficient of air solubility, which is approximately 0.02 at 20 °C. From Boyle's law, the incremental formulation for pore air pressure is determined as

$$\Delta u_a=-(1-\xi)\frac{p_a+u_a}{n_a}\Delta n_a=-P\Delta n_a \tag{7a}$$

$$P=(1-\xi)\frac{p_a+u_a}{n_a} \tag{7b}$$

where p_a is the atmospheric pressure and ξ is the air drainage ratio, which is defined as the ratio of partially drained gas mass to completely drained gas mass, i.e.

$$\xi=\frac{\Delta q_a}{\rho_a\Delta n_a} \tag{8}$$

where Δq_a is the drained gas mass and ρ_a is the pore air density.

When pore air content is changed from initial pore air content n_{a0} to n_a, the pore air pressure is changed from 0 to u_a accordingly. Eq. (7) can be re-written as

$$\frac{\Delta u_a}{u_a+p_a}=-\frac{1-\xi}{n_a}\Delta n_a \tag{9}$$

When the air drainage ratio ξ is constant, integrating the above equation yields the following relationship between pore air pressure and pore air content:

$$u_a=\left[\left(\frac{n_{a0}}{n_a}\right)^{1-\xi}-1\right]p_a \tag{10}$$

where n_{a0} is the initial pore air content, $=[1-(1-c_h)S_{r0}]n_0$, n_0 is the initial porosity and S_{r0} is the initial degree of saturation.

If the air is completely drained,

$$\xi=1,\quad u_a=0 \tag{11}$$

If the air is completely undrained,

$$\xi=0,\quad u_a=\left(\frac{n_{a0}}{n_a}-1\right)p_a \tag{12}$$

From Eq. (6), n_a is a function of S_r and n. By differentiating n_a with respect to S_r and n, we can get

$$\Delta n_a=\frac{\partial n_a}{\partial S_r}\Delta S_r+\frac{\partial n_a}{\partial n}\Delta n=\frac{\partial n_a}{\partial S_r}\frac{\partial S_r}{\partial s}(\Delta u_w-\Delta u_a)+\frac{\partial n_a}{\partial n}\Delta n \tag{13}$$

where

$$\Delta S_r=\frac{\partial S_r}{\partial s}\Delta s=\frac{\partial S_r}{\partial s}(\Delta u_w-\Delta u_a) \tag{14}$$

From Eqs. (7) and (13), we can get

$$\Delta u_a=-\frac{P\frac{\partial n_a}{\partial S_r}\frac{\partial S_r}{\partial s}}{1-P(\partial n_a/\partial S_r)(\partial S_r/\partial s)}\Delta u_w-\frac{P\frac{\partial n_a}{\partial n}}{1-P(\partial n_a/\partial S_r)(\partial S_r/\partial s)}\Delta n \tag{15}$$

For a soil, the change in porosity is equal to the change in volumetric strain, i.e. $\Delta n=\Delta\varepsilon_v$. Substituting Eq. (15) into Eq. (5) yields

$$\Delta\sigma=\Delta\sigma'+A_1\Delta u_w+A_2\Delta\varepsilon_v \tag{16a}$$

where

$$A_1=\frac{\chi+(\partial\chi/\partial s)s-P(\partial n_a/\partial S_r)(\partial S_r/\partial s)}{1-P(\partial n_a/\partial S_r)(\partial S_r/\partial s)},\quad A_2=\frac{(\chi+(\partial\chi/\partial s)s-1)P(\partial n_a/\partial n)}{1-P(\partial n_a/\partial S_r)(\partial S_r/\partial s)} \tag{16b}$$

2.2. Numerical schemes

The continuity equation in consolidation analysis is expressed as

$$\frac{\partial v_x}{\partial x}+\frac{\partial v_y}{\partial y}+\frac{\partial v_z}{\partial z}+\frac{1}{\rho_w}\frac{\partial(\rho_w nS_r)}{\partial t}=0 \tag{17}$$

where v_x, v_y and v_z are the velocities along x, y and z directions respectively and ρ_w is the density of pore water. Then we can get

$$-\frac{1}{\gamma_w}\left[\frac{\partial}{\partial x}\left(k_x\frac{\partial\bar{h}}{\partial x}\right)+\frac{\partial}{\partial y}\left(k_y\frac{\partial\bar{h}}{\partial y}\right)+\frac{\partial}{\partial z}\left(k_z\frac{\partial\bar{h}}{\partial z}\right)\right]+\tilde{S}_r\frac{\partial\varepsilon_v}{\partial t}+S_s\frac{\partial\bar{h}}{\partial t}=0 \tag{18a}$$

$$\tilde{S}_r=S_r+\frac{nP(\partial n_a/\partial n)(\partial S_r/\partial s)}{1-P(\partial n_a/\partial S_r)(\partial S_r/\partial s)},\quad S_s=n\beta S_r-\frac{n(\partial S_r/\partial s)}{1-P(\partial n_a/\partial S_r)(\partial S_r/\partial s)} \tag{18b}$$

where $\bar{h}=\gamma_w h=\gamma_w z-u_w$ and $\beta=(1/\rho_w)(\partial\rho_w/\partial u_w)$.

Hence, the corresponding finite element formulations are obtained:

$$\tilde{S}_r[K_c]^T\{\dot{\delta}\}+[K_s]\{\bar{h}\}\{+[K_p]\{\dot{\bar{h}}\}=-\int[\bar{N}]^T v_n ds \tag{19}$$

where $[K_c]$, $[K_s]$ and $[K_p]$ are computing matrices; $\{\delta\}$ is the deformation matrix; $\{\bar{h}\}$ is the matrix of water head; $(\dot{\bullet})$ denotes partial differentiation with respect to time; $[\bar{N}]$ is the matrix of shape function; and v_n is the flow rate on the boundary.

The incremental expression of Eq. (19) within a time increment $t-\Delta t\sim t$ is

$$\tilde{S}_r[K_c]^T\{\Delta\delta\}+(\theta\Delta t[K_s]^T+[K_p])\{\bar{h}\}=-\Delta t\int[\bar{N}]^T[\theta v_n+(1-\theta)v_{n-1}]ds$$
$$+[K_p]\{\bar{h}_{t-\Delta t}\}-\Delta t(1-\theta)[K_s]_{t-\Delta t}\{\bar{h}_{t-\Delta t}\} \tag{20}$$

where θ is a constant. Its value varies between 0.5 and 1, and is generally 2/3.

The equilibrium equation in consolidation analysis is written as

$$\int [B]^T\{\Delta\sigma\}dV = \{\Delta F\} \tag{21}$$

where $\{\Delta F\}$ is load increment matrix. Eq. (16a) is re-written in matrix form as

$$\{\Delta\sigma\} = \{\Delta\sigma'\} + A_1\{M\}\Delta u_w + A_2\{M\}\{M\}^T\{\Delta\varepsilon\} = [\overline{D}]\{\Delta\varepsilon\} + A_1\{M\}\Delta u_w \tag{22}$$

where

$$[\overline{D}] = [D] + A_2\{M\}\{M\}^T \tag{23a}$$

$$\{M\} = \{\,1 \quad 1 \quad 1 \quad 0 \quad 0 \quad 0\,\}^T \tag{23b}$$

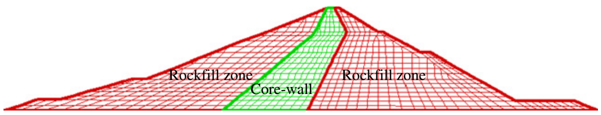

Fig. 1. FEM mesh of a core-wall dam.

Table 1
Degree of saturation, relative permeability coefficient and suction of the rockfill material.

Suction, s (kPa)	Degree of saturation, S_r	Relative permeability coefficient, k_r
0	1	1
5.38	0.79	0.32
12.3	0.39	0.012
17.7	0.32	1.3e-3
23.8	0.29	1.6e-4
37.7	0.25	4.0e-5
68.9	0.22	1.3e-5
100	0.20	1.0e-5
200	0.17	2.3e-6
500	0.15	5.2e-7
1000	0.13	1.3e-8
1500	0.13	3.2e-10

Table 2
Degree of saturation, relative permeability coefficient and suction of the core-wall material.

Suction, s (kPa)	Degree of saturation, S_r	Relative permeability coefficient, k_r
0	1	1
16.4	0.95	0.61
21.2	0.9	0.38
29.2	0.825	0.14
44.8	0.75	0.054
61.2	0.70	0.027
85.6	0.65	0.014
140	0.575	6.3e-3
210	0.50	2.9e-3
330	0.425	1.2e-3
940	0.35	1.3e-4
1440	0.325	1.0e-4

Substituting Eq. (22) into Eq. (21) and taking into account $\Delta\overline{h} = -\Delta u_w$ yield

$$[K]\{\Delta\delta\} - A_1[K_c]\{\Delta\overline{h}\} = \{\Delta F\} \tag{24a}$$

where $[K]$ is stiffness matrix. By considering $\Delta\overline{h} = \overline{h}_t - \overline{h}_{t-\Delta t} = \overline{h} - \overline{h}_{t-\Delta t}$, we can get

$$[K]\{\Delta\delta\} - A_1[K_c]\{\overline{h}\} = \{\Delta F\} - A_1[K_c]\{\overline{h}\}_{t-\Delta t} \tag{24b}$$

To maintain the symmetry of coefficient matrix when Eq. (24b) is grouped with Eq. (20) as simultaneous equations, $A_1[K_c]\{\overline{h}\}$ is revised as $\tilde{S}_r[K_c]\{\overline{h}\} + (A_1 - \tilde{S}_r)[K_c]\{\overline{h}\}$. Subsequently, Eq. (24b) is further re-written as

$$[K]\{\Delta\delta\} - \tilde{S}_r[K_c]\{\overline{h}\} = \{\Delta F\} + [K_c][(A_1 - \tilde{S}_r)\{\overline{h}\} - A_1\{\overline{h}\}_{t-\Delta t}] \tag{25}$$

Eqs. (25) and (20) can be solved together. Iterative calculation is required due to the unknown quantity $\overline{h}$ on the right-hand side of Eq. (25).

3. Results

The simplified consolidation approach for unsaturated soils better corresponds to reality than that for saturated soils regarding numerical simulations of earth-rock dams. At the same time, computational complexity is not increased too much. So it is very feasible in carrying out numerical analysis of earth-rock dams.

Fig. 1 shows the mesh of the cross-section of a high core-wall dam. The bottom elevation of the mesh is 142 m and the top elevation is 283 m. Upstream side is on the left and the highest water level is 278 m. Downstream side is on the right and the water level is kept at zero.

As shown in Fig. 1, the core-wall is located in the central zone and its two sides are rockfill zones. The saturated permeability of the core-wall material is 8.64×10^{-5} m/d (i.e., 1.0×10^{-7} cm/s) and that of rockfill material is 86.4 m/d (i.e., 0.1 cm/s). The degree of saturation and relative permeability coefficient of the two materials are provided in Tables 1 and 2 (Wu, 1998).

The parameter χ in Eq. (1) is related to suction as suggested by Khalili and Khabbaz (1998)

$$\chi = (s/s_e)^{-m}, \text{ if } s \geq s_e; \quad \chi = 1, \text{ if } s < s_e \tag{26}$$

where s_e is air entry value and m is a constant (usually its value is 0.55).

The constitutive model proposed by Shen and Zhang (1988) is used in this study. The deformation modulus in this model is similar to that in Duncan–Chang's model (Duncan and Chang, 1970), i.e.,

$$E_t = \left[1 - \frac{R_f(1-\sin\phi)(\sigma_1-\sigma_3)}{2c\cos\phi + 2\sigma_3\sin\phi}\right]^2 KP_a\left(\frac{\sigma_3}{P_a}\right)^n \tag{27}$$

Different from Duncan–Chang's model, the Poisson ratio in this model is calculated as

$$\mu_t = \frac{1}{2} - c_d\left(\frac{\sigma_3}{p_a}\right)^{n_d} \frac{E_i R_f}{(\sigma_1-\sigma_3)_f} \frac{1-R_d}{R_d}\left(1 - \frac{R_f S_l}{1-R_f S_l}\frac{1-R_d}{R_d}\right) \tag{28}$$

where $E_i = KP_a(\sigma_3/P_a)^n$; c_d, n_d, R_d are parameters.

The parameters of constitutive model used in this analysis are shown in Table 3.

Table 3
Parameters for the core-wall dam.

Item	c (kPa)	ϕ_0 (deg.)	$\Delta\phi$ (deg.)	R_f	K	n	c_d	n_d	R_d
Upstream rockfill zone	0	50.8	7.36	0.63	766	0.44	0.0038	0.727	0.658
Core-wall	20	28	0	0.71	256	0.27	0.0039	1.217	0.802
Downstream rockfill zone	0	40	5	0.78	750	0.50	0.0038	0.727	0.658

The values of other relevant parameters are set as follows. For the rockfill material, the unit weight is 21 kN/m^3, the initial porosity 0.20, the initial degree of saturation 0.29, the air entry value s_e=20 kPa, the constant m=0.55, and ξ=1. For the core-wall material, the unit weight is 20 kN/m^3, the initial porosity 0.38, the initial degree of saturation 0.90, the air entry value s_e=20 kPa, the constant m=0.55, and ξ=1.

The simulated process includes the construction of dam and subsequent increasing of upstream water level to 278 m. The rate of dam construction is 0.2 m/d, i.e., 1 m rise per five days. During the water filling, the rate of water level increase is 0.5 m/d, i.e., 1 m rise per two days.

Fig. 2 shows the contour lines of stress, displacement and pore water pressure on the completion of dam construction. Fig. 3 shows the results as water level climbs to the elevation of 278 m. Fig. 4 shows the results after 10 years of water filling.

Figs. 5–10 show the computation results by decreasing soil modulus to 2/3 and 1/2, i.e., replacing K in Eq. (27) with (2/3)K and (1/2)K, respectively. It is found that as soil modulus decreases, the deformation of dam becomes larger and the corresponding phreatic line and pore water pressures are higher. The coupling effect among pore water pressure, soil modulus and deformation is obvious.

Fig. 11 shows the variations of phreatic line within the core-wall computed from unsaturated seepage analysis in which the coupling effect between deformation and pore water pressure is not considered. From left to right, this figure shows the phreatic lines at 0th year, 0.5th year, 3rd year, 10th year, 20th year, 50th year, 100th year and 200th year after the water level reaches the elevation of 276 m. It is found that due to the extremely low permeability of core-wall material, the seepage may stabilize until after 200 years. In the coupled analysis with simplified consolidation approach, the pore water pressure increases because of the deformation of core-wall as well as the seepage of the water, hence the rising of phreatic line is quicker as

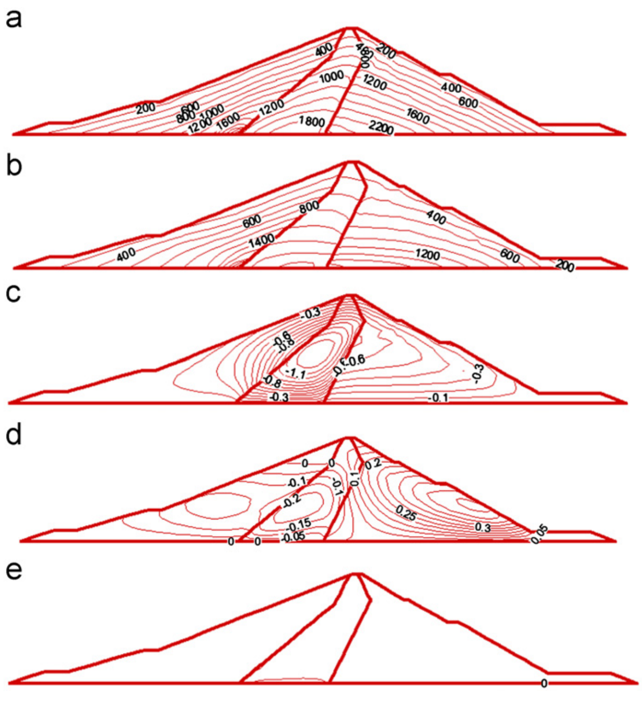

Fig. 2. Contour lines of stress, displacement and pore water pressure on the completion of dam construction. (a) Vertical effective stress (unit: kPa). (b) Horizontal effective stress (unit: kPa). (c) Vertical displacement (unit: m). (d) Horizontal displacement (unit: m). (e) Pore water pressure (unit: kPa).

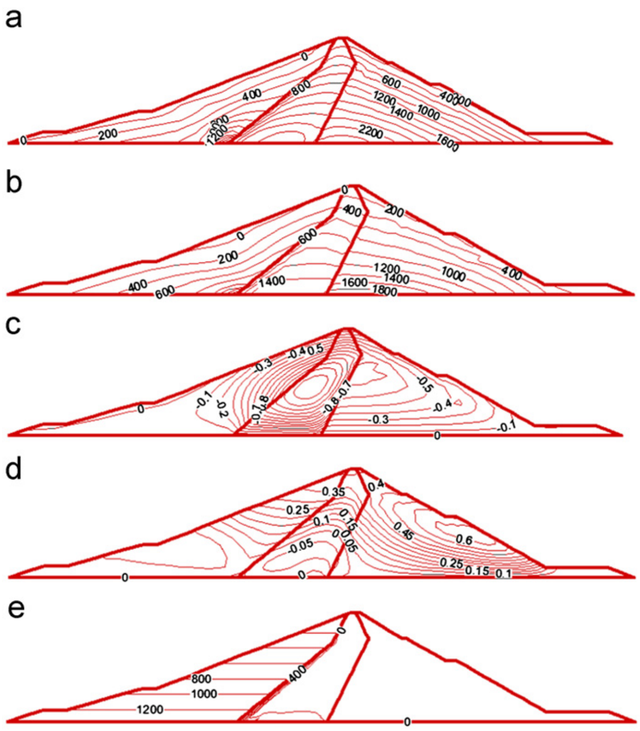

Fig. 3. Contour lines of stress, displacement and pore water pressure when the upstream water level climbs to 278 m elevation. (a) Vertical effective stress (unit: kPa). (b) Horizontal effective stress (unit: kPa). (c) Vertical displacement (unit: m). (d) Horizontal displacement (unit: m). (e) Pore water pressure (unit: kPa).

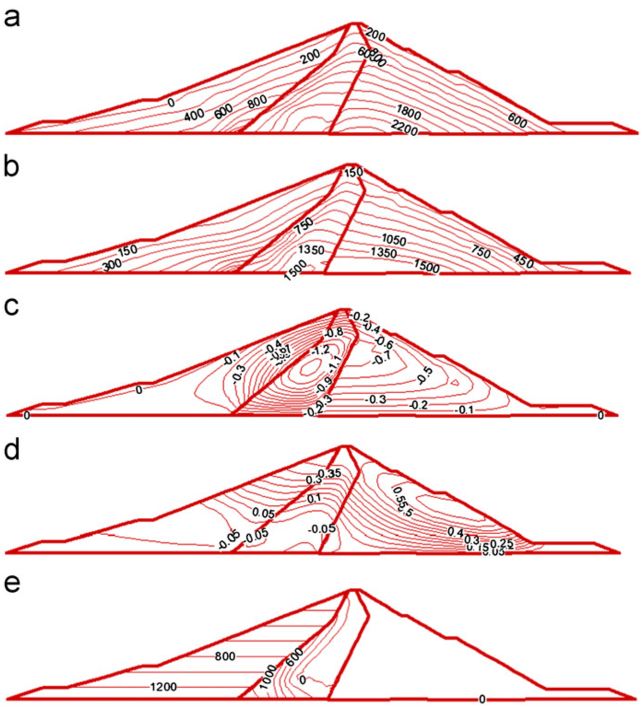

Fig. 4. Contour lines of stress, displacement and pore water pressure after 10 years of keeping upstream water level at 278 m elevation. (a) Vertical effective stress (unit: kPa). (b) Horizontal effective stress (unit: kPa). (c) Vertical displacement (unit: m). (d) Horizontal displacement (unit: m). (e) Pore water pressure (unit: kPa).

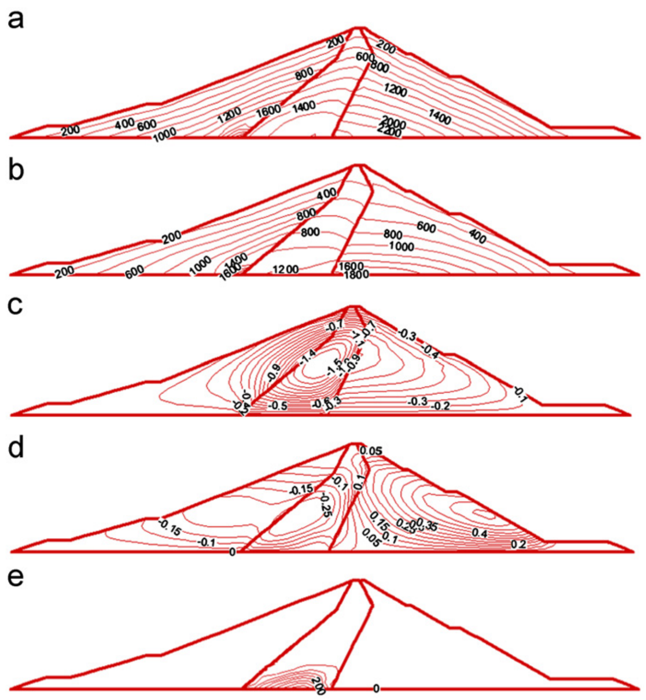

Fig. 5. Contour lines of stress, displacement and pore water pressure on the completion of dam construction (2/3K). (a) Vertical effective stress (unit: kPa). (b) Horizontal effective stress (unit: kPa). (c) Vertical displacement (unit: m). (d) Horizontal displacement (unit: m). (e) Pore water pressure (unit: kPa).

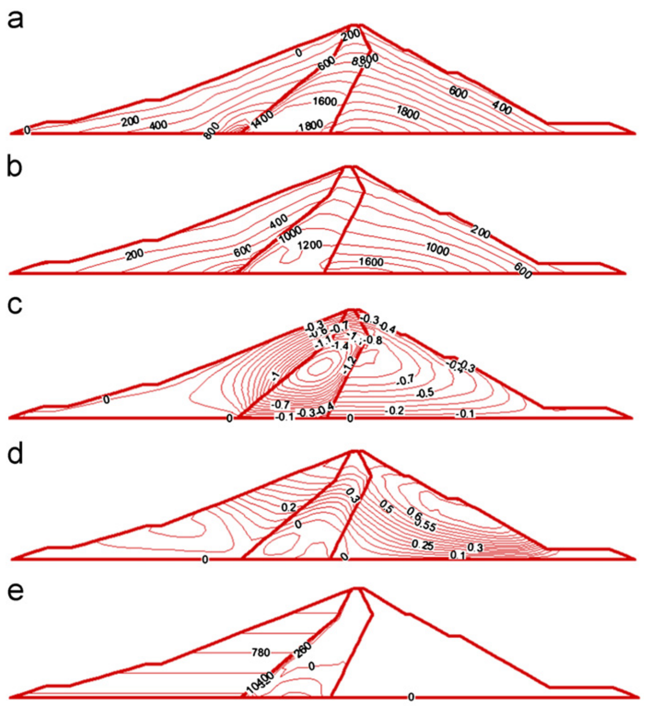

Fig. 6. Contour lines of stress, displacement and pore water pressure when the upstream water level climbs to 278 m elevation (2/3K). (a) Vertical effective stress (unit: kPa). (b) Horizontal effective stress (unit: kPa). (c) Vertical displacement (unit: m). (d) Horizontal displacement (unit: m). (e) Pore water pressure (unit: kPa).

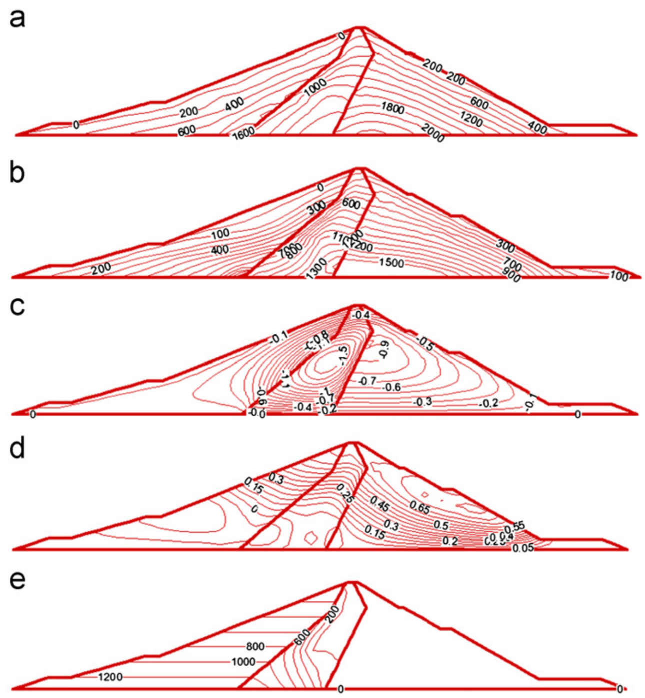

Fig. 7. Contour lines of stress, displacement and pore water pressure after 10 years of keeping upstream water level at 278 m elevation (2/3K). (a) Vertical effective stress (unit: kPa). (b) Horizontal effective stress (unit: kPa). (c) Vertical displacement (unit: m). (d) Horizontal displacement (unit: m). (e) Pore water pressure (unit: kPa).

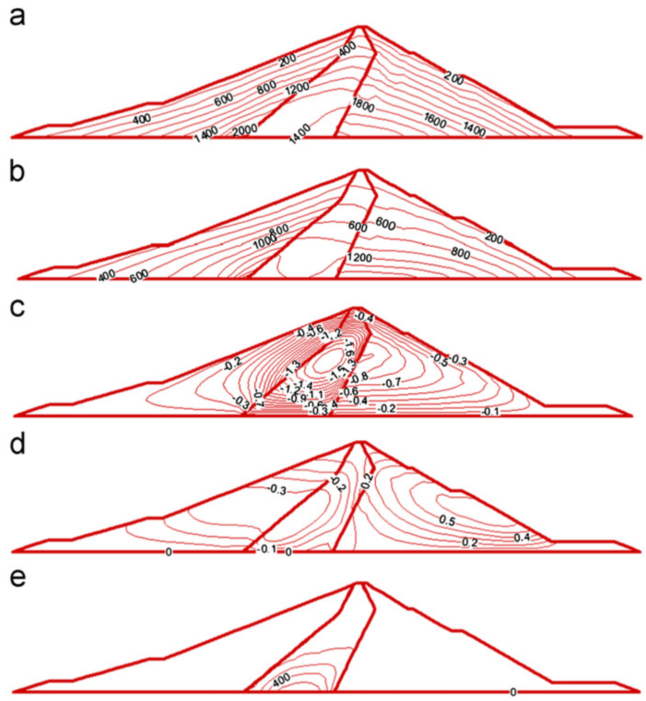

Fig. 8. Contour lines of stress, displacement and pore water pressure on the completion of dam construction (1/2K). (a) Vertical effective stress (unit: kPa). (b) Horizontal effective stress (unit: kPa). (c) Vertical displacement (unit: m). (d) Horizontal displacement (unit: m). (e) Pore water pressure (unit: kPa).

compared with the uncoupled analysis. That is to say, the pore water pressure at the bottom of core-wall is related not only to the unsaturated seepage caused by change of water level, but also to the excess pore water pressure induced by deformation. As soil modulus decreases, the deformation of dam becomes larger and the rising of phreatic line is quicker.

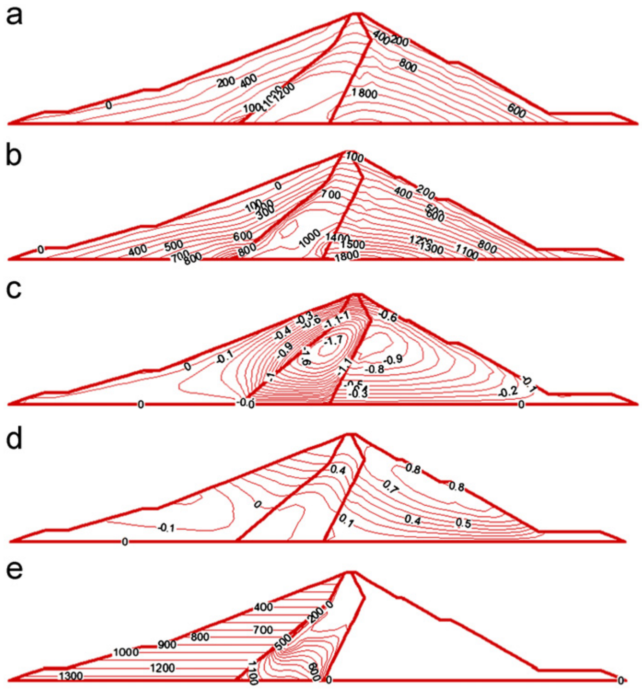

Fig. 9. Contour lines of stress, displacement and pore water pressure when the upstream water level climbs to 278 m elevation (1/2K). (a) Vertical effective stress (unit: kPa). (b) Horizontal effective stress (unit: kPa). (c) Vertical displacement (unit: m). (d) Horizontal displacement (unit: m). (e) Pore water pressure (unit: kPa).

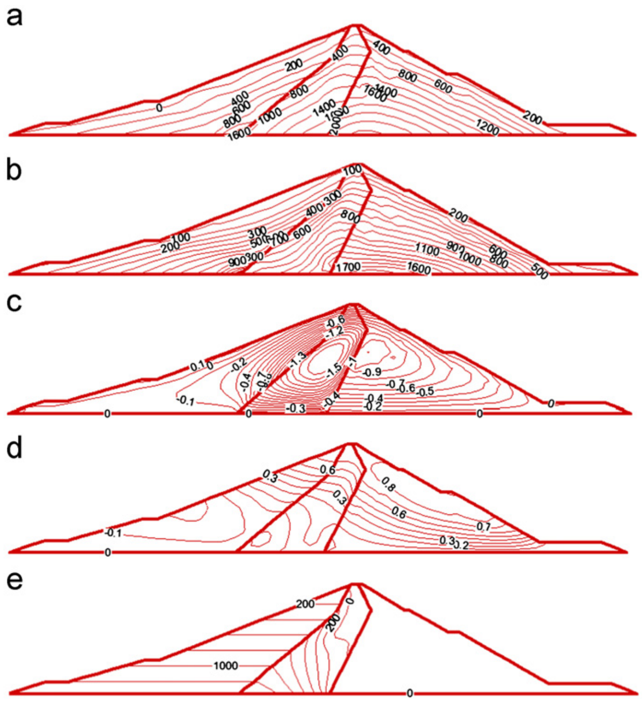

Fig. 10. Contour lines of stress, displacement and pore water pressure after 10 years of keeping the upstream water level at 278 m elevation (1/2K). (a) Vertical effective stress (unit: kPa). (b) Horizontal effective stress (unit: kPa). (c) Vertical displacement (unit: m). (d) Horizontal displacement (unit: m). (e) Pore water pressure (unit: kPa).

Additionally, the parameter K in Eq. (27) is increased by 1.5 and 2.0 times to compute variations of stress, displacement and pore water pressure. Fig. 12 shows the contour lines of pore

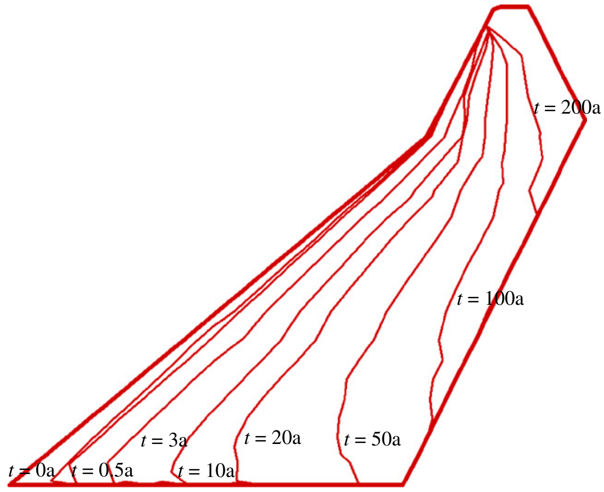

Fig. 11. Variations of phreatic line computed from unsaturated seepage analysis at different times after the upstream water level reaches 278 m elevation.

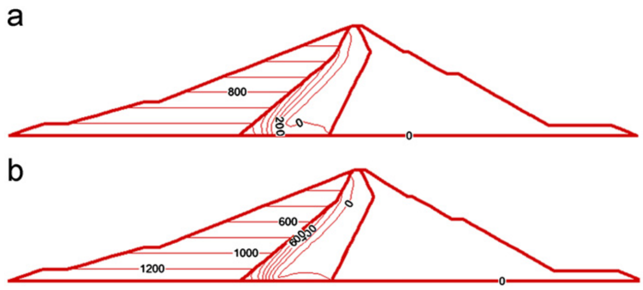

Fig. 12. Contour lines of pore water pressure after 10 years of keeping the upstream water level at 278 m elevation (computed by using different values of soil modulus). (a) 1.5 K and (b) 2.0 K.

water pressure after 10 years of keeping the upstream water level at 278 m elevation. The results show that as the soil modulus increases, the coupling effect between deformation and excess pore water pressure becomes weaker and thus the computed phreatic line is more close to that computed from unsaturated uncoupled seepage analysis.

4. Conclusions

In this study, a simplified approach for consolidation analysis of unsaturated soil is applied to numerical simulation of an earth-rock dam during the process of water-filling. The computational results include stress and displacement fields within the dam and the variations of pore water pressure and phreatic line. The results show that due to the coupling effect between deformation and pore water pressure, the development of pore water pressure in the core-wall of the dam is quicker than that computed from unsaturated seepage analysis without coupling deformation. As soil modulus decreases, the deformation of the dam becomes larger and the coupling effect is stronger, leading to quicker development of pore water pressure and phreatic line. The variations of pore water pressure within the core-wall are related not only to unsaturated seepage induced by variations of water level, but also to the excess pore water pressure induced by deformation. These may explain why there is high water pressure measured shortly after the completion of earth-rock dam.

It should be noted that the computations of transient seepage for unsaturated soils are difficult to converge as compared with steady seepage analysis due to iterative calculations related to a variety of factors such as phreatic line, permeability coefficient and soil modulus. The computational parameters should be in line with engineering practice. Extreme values of permeability coefficient and of parameters of constitutive model may aggravate computational convergence and meaningful results are not likely to be achieved.

Acknowledgments

The supports of Natural Science Foundation of China (51039003), National Basic Research Program of China (973 Program 2010CB732103), and the State Key Laboratory of Hydroscience and Engineering (2012-KY-02) are gratefully acknowledged.

References

Barden, L., 1965. Consolidation of compacted and unsaturated clays. Geotechnique 15 (3), 267–286.
Bathe, K.J., Khoshgoftaar, M.R., 1979. Finite element free surface seepage analysis without mesh iteration. International Journal for Numerical and Analytical Methods in Geomechnics 3, 13–22.
Biot, M.A., 1941. General theory of three-dimensional consolidation. Journal of Applied Physics 12 (2), 155–164.
Bishop, A.W., 1959. The principle of effective stress. Teknisk Ukeblad 106 (39), 859–863.
Darbandi, M., Torabi, S.O., Saadat, M., Daghighi, Y., Jarrahbashi, D., 2007. A moving-mesh finite-volume method to solve free-surface seepage problem in arbitrary geometries. International Journal for Numerical and Analytical Methods in Geomechnics 31, 1609–1629.
Deng, G., Shen, Z.J., 2006. Numerical simulation of crack formation process in clays during drying and wetting. Geomechanics and Geoengineering 1 (1), 27–43.
Deng, G., Shen, Z.J., Chen, T.L., Yang, D.Q., 2003. Numerical simulation of slope failure during/after rainfall. Proceeding of International Conference on Slope Engineering, Hong Kong, pp. 207–212.
Deng, G., Shen, Z.J., Yang, D.Q., 2006. Numerical simulation of crack formation due to desiccation in the clay surface. Chinese Journal of Geotechnical Engineering 28 (2), 241–248. (in Chinese).
Desai, C.S., 1976. Finite element residual schemes for unconfined flow. International Journal for Numerical Methods in Engineering 10, 1415–1418.
Duncan, J.M., Chang, C.Y., 1970. Nonlinear analysis of stress and strain in soils. Journal of Soil Mechanics and Foundation Division 96 (5), 1629–1653.
Fredlund, D.G., Hasan, J.U., 1979. One-dimensional consolidation theory for unsaturated soils. Canadian Geotechnical Journal 17 (3), 521–531.
Fredlund, D.G., Morgenstern, N.R., 1976. Constitutive relations for volume change in unsaturated soils. Canadian Geotechnical Journal 13 (2), 386–396.
Fredlund, D.G., Rahardjo, H., 1993. Soil Mechanics for Unsaturated Soil. John Wiley and Sons Inc., New York.
Jiang, Q.H., Deng, S.S., Zhou, C.B., Lu, W.B., 2010. Modeling unconfined seepage flow using three-dimensional numerical manifold method. Journal of Hydrodynamics 22 (4), 554–561.
Jie, Y.X., Jie, G.Z., Mao, Z.Y., Li, G.X., 2004. Seepage analysis based on boundary-fitted coordinate transformation method. Computers and Geotechnics 31 (4), 279–283.
Khalili, N., Khabbaz, M.H., 1998. A unique relationship for x for the determination of the shear strength of unsaturated soils. Geotechnique 48 (5), 681–687.
Lam, L., Fredlund, D.G., 1984. Saturated–unsaturated transient finite element seepage model for geotechnical engineering. Advances in Water Resources 7, 132–136.
Li, G.X., Ge, J.H., Jie, Y.X., 2003. Free surface seepage analysis based on the element-free method. Mechanical Research Communication 30, 9–19.
Lloret, A., Alonso, E.E., 1980. Consolidation of unsaturated soils including swelling and collapse behavior. Geotechnique 30 (4), 449–477.
Sandhu, R.S., Wilson, E.L., 1969. Finite element analysis of seepage in elastic media. Journal of the Engineering Mechanics Division 95 (3), 641–652.
Scott, R.F., 1963. Principles of Soil Mechanics. Addison Wesley Publishing Company.
Shen, Z.J., 2003. Simplified consolidation theory for unsaturated soils and its application. Hydro-Science and Engineering 12 (4), 1–6. (in Chinese).
Shen, Z.J., Zhang, W.M., 1988. Analysis of effective stress and movements of Lubuge dam, Numerical Methods in Geomechanics: Innsbruck, 1988, Proceeding of the 6th International Conference on Numerical Methods in Geomechanics. Balkema, Rotterdam.
Wu, M.X., 1998. The Coupled Analysis Method of Seepage and Deformation of Unsaturated Soils and its Application in Earth Cored Rockfill Dam. Ph.D. Thesis. Tsinghua University, Beijing (in Chinese).
Zheng, H., Liu, D.F., Lee, C.F., Tham, L.G., 2005. A new formulation of Signorini's type for seepage problems with free surfaces. International Journal for Numerical Methods in Engineering 64 (1), 1–16.